Editors' choice

Evidence for different shark species feeding on a diminutive right whale and a relative of the beluga in the Early Pliocene of the southern North Sea

OLIVIER LAMBERT, JOHN R. STEWART, STEPHEN LOUWYE, LUC DE CONINCK, MARK BOSSELAERS, LUCILE CRÉTÉ, STIJN GOOLAERTS, CHRISTOPHE MALLET, and FREDERIK H. MOLLEN

Lambert, O., Stewart, J.R., Louwye, S., De Coninck, L., Bosselaers, M., Crété, L., Goolaerts, S., Mallet, C., and Mollen, F.H. 2026. Evidence for different shark species feeding on a diminutive right whale and a relative of the beluga in the Early Pliocene of the southern North Sea. *Acta Palaeontologica Polonica* 71 (1): 69–84.

Documenting past trophic relationships is crucial to understand deep time changes in the ecology and geographic distribution of large marine predators. Though bite marks on cetacean bones are a useful source of information to assess shark-whale predator-prey relationships, in many cases the identity of the prey and/or predator cannot be precisely determined. In this work, we investigate two cetacean specimens from the Kattendijk Formation (Lower Pliocene, north of Belgium): (i) the partial cranium of a small balaenid (right whale) that we describe and refer to *Balaenella brachyrhynus* and (ii) the previously described partial skeleton of a monodontid (family of beluga and narwhal), attributed here to the genus *Casatia*. Shark bite marks observed on the bones of the two specimens are described and the tip of a shark tooth found embedded in each cranium is visualized through micro-CT imaging. A comparison with shark species recorded in the Kattendijk Formation allows for the identification of the author of at least one bite for each cetacean: the bluntnose sixgill shark *Hexanchus griseus* for *B. brachyrhynus* and the large lamnid shark *Carcharodon plicatilis* for *Casatia* sp. Based on the position and topology of the marks, the *H. griseus* bite on *B. brachyrhynus* may have occurred on an upside down, floating carcass, a hypothesis that could indicate a scavenging event. Bite marks on the monodontid cranium suggest an attempt by *C. plicatilis* to sever the head from the rest of the body and point to the forehead region as a main targeted area. These new Early Pliocene records of shark-cetacean trophic relationships constitute a first step towards the exploration of the possible link between changes through time in the availability of prey in the southern North Sea and the local loss of large predatory sharks, which occurred in the Late Pliocene to Pleistocene time interval.

Key words: Mammalia, Balaenidae, Monodontidae, *Carcharodon*, *Hexanchus*, trophic interaction, active predation, scavenging, Belgium.

Olivier Lambert [olambert@naturalsciences.be; ORCID: https://orcid.org/0000-0003-0740-5791] and Stijn Goolaerts [sgoolaerts@naturalsciences.be; ORCID: https://orcid.org/0000-0002-7082-9012], O.D. Earth & History of Life, Royal Belgian Institute of Natural Sciences, Vautierstreet 29, 1000 Brussels, Belgium.
John R. Stewart [jstewart@bournemouth.ac.uk; ORCID: http://orcid.org/0000-0002-3506-5264], Faculty of Health, Environment and Medical Sciences, Bournemouth University, Fern Barrow, Poole, BH12 5BB Dorset, UK.
Stephen Louwye [stephen.louwye@ugent.be; ORCID: https://orcid.org/0000-0003-4814-4313], Department of Geology, Ghent University, Krijgslaan 297/S8, 9000 Ghent, Belgium.
Luc De Coninck [deconinckluc11@outlook.be], Belgische Vereniging voor Paleontologie, Belgische Vereniging voor Paleontologie, Lage Kerkwegel 3, 9170 Sint-Gillis-Waas, Belgium.
Mark Bosselaers [mark.bosselaers@telenet.be; ORCID: https://orcid.org/0000-0003-3016-1246], O.D. Earth & History of Life, Royal Belgian Institute of Natural Sciences, Brussels, Belgium; Koninklijk Zeeuwsch Genooschap der Wetenschappen, Kousteensedijk 7, 4331 Middelburg, The Netherlands.
Lucile Crété [l.crete@nhm.ac.uk; ORCID: https://orcid.org/0000-0001-8460-7747], Centre for Human Evolution Research, Natural History Museum, Cromwell Road, SW7 5BD London, UK.
Christophe Mallet [cmallet@naturalsciences.be; ORCID: https://orcid.org/0000-0002-1982-3803], O.D. Earth & History of Life, Royal Belgian Institute of Natural Sciences, Brussels, Belgium; Faculty of Engineering, Department of Geology and Applied Geology, University of Mons, rue de Houdain 9, 7000 Mons, Belgium.
Frederik H. Mollen [frederik.mollen@gmail.com; ORCID: https://orcid.org/0000-0002-9934-1029], Elasmobranch Research, Rehaegenstraat 4, 2820 Bonheiden, Belgium.

Received 8 October 2025, accepted 25 November 2025, published online 18 March 2026.

Introduction

The geographic distribution of large marine predators is driven by many parameters, including prey preferences and prey availability (e.g., Receveur et al. 2022; Afonso et al. 2022). For a better understanding of changes in predator distribution patterns and, more generally, of their ecology, it is therefore crucial to document trophic relationships. In modern oceans, many large sharks are reported to feed, either via active predation or scavenging, on various cetacean species, and such interactions are proposed based on direct sightings of predation/scavenging behaviours, shark stomach contents, bite marks on cetacean carcasses or on the body of survivors, and stable isotope analyses (Corkeron et al. 1987; Long and Jones 1996; Heithaus 2001; MacNeil et al. 2012; Tucker et al. 2019; Nielsen et al. 2019; Assemat et al. 2024; Mucientes et al. 2025).

Although some shark fossil skeletons have been found with fossilized digestive tract contents (e.g., Shimada 1997; Collareta et al. 2017b; Klug et al. 2021), most are from Mesozoic and early Cenozoic strata, and none have provided support for past trophic interactions between sharks and cetaceans. By far, the main source of information remains the description of bite marks on cetacean fossil bones (e.g., Bianucci et al. 2010; Govender and Chinsamy 2013; Collareta et al. 2017a; Godfrey et al. 2018; Benites-Palomino et al. 2023).

In addition to the difficulties faced to distinguish between active predation on living animals and scavenging on dead carcasses, it is often challenging to identify the most likely candidate for the bite marks because the shape and distribution of the marks are often not conclusive. Shark tooth fragments embedded in bone could provide further clues, but such findings are relatively scarce in the fossil record (Godfrey et al. 2025 and references therein). On the other hand, the identity of the attacked cetacean is also often difficult to assess due to the fragmentary/non-diagnostic state of the preserved bones (e.g., Ehret et al. 2009; Govender and Chinsamy 2013; Godfrey et al. 2021, 2025). Therefore, cases for which both the shark and the cetacean are tentatively identified at the genus or species level remain rare (e.g., Deméré and Cerutti 1982; Cigala-Fulgosi 1990; Bianucci et al. 2010; Collareta et al. 2017a).

For the whole Neogene of the southern North Sea, despite a relatively rich record of cetaceans, in addition to the brief mention of bite marks on the bones of an Early Pliocene balaenopterid (rorqual) and alate Pliocene balaenid (right whale) (Bisconti and Bosselaers 2016; Duboys de Lavigerie et al. 2020), only a partial skeleton of a monodontid (a relative of the modern beluga and narwhal) from the Lower Pliocene of the Port of Antwerp (Belgium) has been described with shark bite marks on the cranium (Lambert and Gigase 2007). Though the species identity of the shark producing the marks could not be firmly established, the depth and spacing of the marks, as well as a tooth tip deeply embedded in the bone, indicated a powerful and large shark, possibly an extinct mako shark *Cosmopolitodus hastalis* (here identified as *Carcharodon plicatilis* or *Caracharodon hastalis*, broad form), although the Greenland shark *Somniosus microcephalus* was also mentioned in the discussion about the possible author of the marks (Lambert and Gigase 2007). In the current analysis, we reassess the systematic affinities of the monodontid whale, the bite marks are redescribed, and the morphology of the embedded shark tooth tip is investigated via micro-CT scanning.

In addition to the forementioned skeleton, a recently acquired partial cranium of a small balaenid (a relative of the modern right whales and bowhead), also from the Early Pliocene of the Port of Antwerp, displays a series of bite marks and a tooth tip embedded in the occipital shield. As for the monodontid, the systematics of the balaenid cranium are discussed, and the bite marks and tooth tip are analyzed (also via micro-CT scanning for the latter). These investigations allow for the interpretation of the selachians responsible for the bites on these two whale crania, thus enriching our knowledge of a key aspect of shark and cetacean palaeoecology in the southern North Sea, namely their past trophic relationships.

Institutional abbreviations.—NMB, Natuurmuseum Brabant, Tilburg, The Netherlands; RBINS, Royal Belgian Institute of Natural Sciences, Brussels, Belgium; USNM, National Museum of Natural History, Smithsonian Institution, Washington, D.C., USA.

Material and methods

Shark bite mark typology.—Bite mark types I-V (TI-TV) and related interpretations of impact types follow Collareta et al. (2017a), modified from Cigala-Fulgosi (1990) (see further details in the description below for the types recorded in this study). For an alternate, more inclusive terminology of bite marks on bone based on ichnotaxonomy (ichnogenus *Linichnus*), see Muñiz et al. (2020).

X-ray computed tomography (micro-CT).—Cranial fragments of the monodontid (RBINS M.1922) and *Balaenella brachyrhynus* Bisconti, 2005 (RBINS M.2344) were digitized using the RBINS micro-CTRX EasyTom 150 of RX Solutions (Chavanod, France), at 19.89 and 31.09 µm respectively, in a single 360° rotation split into 1440 steps. RBINS M.1922 was imaged in small spot mode, with a stainless steel 0.4 mm thick filter, an average of 7 frames per radiograph, and with beam settings at 10W, 126 kV and 79µA, RBINS M.2344 in middle spot mode, with a double 0.4 mm Cu filter, an average of 5 frames per radiograph, and with beam settings at 30 W, 150 kV and 200 µA. Extraction into 16bit tiff stack was performed with X-Act. Visualization, measurements, and segmentation of the shark tooth fragments embedded in the cetacean bones were executed with Dragonfly ORS (2024.1). Extracted meshes (of the shark

tooth fragments) were also studied and optimized (e.g., smoothed) in GOM Inspect.

Additional metadata on the specimens can be found on the RBINS Virtual Collections platform. The original micro-CT imaging data may be obtained upon request from the RBINS Palaeontology Collection Manager.

Surface scanning.—The cranium of the holotype of *Balaenella brachyrhynus* Bisconti, 2005 (NMB 42001) was surface-scanned with an Artec Eva structured-light scanner and the software Artec Studio Professional (v.16, Artec 3D 2018 *Artec Studio Professional*. Available at https://www.artec3d.com/3d-software/artec-studio). The specimen was scanned using the High Definition (HD) mode, with a HD-frames frequency of 1/4 and a HD-data density of 4. HD frames were used to compute HD scans, onto which artifacts and unwanted elements were erased before the scans being aligned. Scans were fused to create a 3D mesh. Potential holes were filled with the "watertight" option, and the "small object" filter was used to remove small artifacts. Texture was computed with an output size of 8192×8192 pixels. The final textured 3D model was exported into ".ply" format.

Palynological analysis.—A sample of partly indurated sediment taken from the cranium RBINS M.2344 was subjected to palynological analysis with dinoflagellate cysts to determine the relative age of the sediments from which this specimen was recovered. The sample was processed using standard laboratory techniques described in Louwye et al. (2004), involving the removal of carbonates with hydrochloric acid (HCl) and silicates with hydrofluoric acid (HF). The residues were filtered on a 16 μm nylon screen and strew mounted on microscope slides with glycerine jelly. The dinoflagellate cysts were analysed with a ZEISS Axioimager A1 light microscope at 200× and 400× magnifications. The presence and numbers of acritarchs, green algae, pollen, spores, invertebrate remains and other *incertae sedis* were noted during the systematic count in non-overlapping traverses.

Results of the palynological analysis and lithostratigraphic origin of RBINS M.2344

The sediment sample yielded a relatively poorly preserved palynomorph assemblage. Many specimens, particularly the thin-walled ones, were often torn or folded. The systematic screening resulted in the identification of only 135 dinoflagellate cyst specimens and 104 bisaccate pollen grains (see SOM: table 1, Supplementary Online Material available at http://app.pan.pl/SOM/app71-Lambert_etal_SOM.pdf), numbers insufficient for a statistically valid analysis. A total of 21 dinoflagellate cyst species and three acritarch species were recorded. Of these, five dinoflagellate cyst species are considered biostratigraphic markers: *Baticasphaera minuta*, *Corrudinium devernaliae*, *Operculodinium tegillatum*, *Reticulatosphaera actinocoronata*, and *Melitasphaeridium choanophorum*.

De Schepper and Head (2008) reported the calibrated highest occurrences of *B. minuta*, *C. devernaliae*, and *O. tegillatum* in DSDP Hole 610A in the eastern North Atlantic at 3.83 Ma, 3.9 Ma, and 3.71 Ma, respectively (Zanclean, Early Pliocene). According to De Schepper et al. (2009), both *R. actinocoronata* and *M. choanophorum* have their highest occurrences in the Zanclean (Lower Pliocene) Kattendijk Formation of the Tunnel Kanaaldok (Antwerp area, northern Belgium), and do not occur in the overlying Lillo Formation. However, the aforementioned species are also known to occur in Upper Miocene deposits.

The lower age boundary of the sample is constrained by the presence of *Achomosphaera andalousiensis andalousiensis*, a subspecies with its lowest occurrence dated to 12.3 Ma (early Serravallian; Dybkjær and Piasecki 2010). The relative age range of the sample can be further narrowed by the absence of *Labyrinthodinium truncatum truncatum* (highest occurrence ~7.6 Ma, late Tortonian) and *Selenopemphix armageddonensis*(highest occurrence ~5 Ma, earliest Zanclean) (Dybkjær and Piasecki 2010).

The sediment sample can thus be associated with the Zanclean Kattendijk Formation (Deckers and Louwye 2020) of northern Belgium (5.0–4.4 Ma; De Schepper et al. 2009).

Systematic palaeontology

Order Cetacea Brisson, 1762
Neoceti Fordyce & Muizon, 2001
Suborder Mysticeti Cope, 1891
Family Balaenidae Gray, 1825
Genus *Balaenella* Bisconti, 2005

Type species: *Balaenella brachyrhynus* Bisconti, 2005; Zanclean (Pliocene), Belgium.

Balaenella brachyrhynus Bisconti, 2005

Figs. 2, 3, 5.

Holotype: NMB 42001, subcomplete cranium.

Type locality: Eerste Kanaaldok (= part of Waaslandkanaal; Smitz 2011; Fig. 1), Kallo, NW Antwerp, Belgium (Bisconti 2005).

Type horizon: Kattendijk Formation, Zanclean (Pliocene) (5.0–4.4 Ma; De Schepper et al. 2009).

Material.—RBINS M.2344, partial neurocranium including part of the supraoccipital, parietals, frontals, a fragment of the right maxilla, and some detached elements of the basicranium and palate, including portions of the vomer (Figs. 2, 3). RBINS M.2344 was discovered ex situ in Pliocene sediment by JRS and Robert O. Stewart around 1984–1985, upon the construction of the Vierde Havendok on the left bank

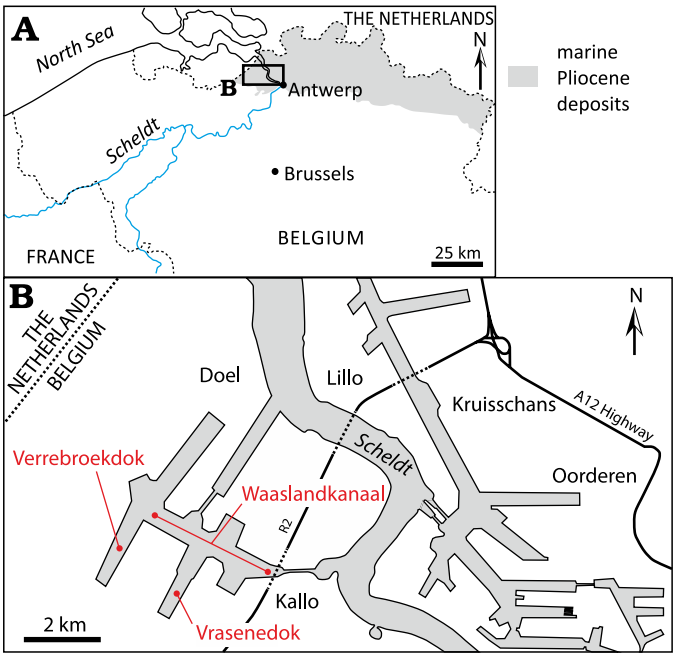

Fig. 1. **A**. Location of the Port of Antwerp area on a map of northern Belgium. Grey shading indicates occurrence of marine Pliocene deposits. **B**. Sketch of the Port of Antwerp indicating the locations where the main fossil cetacean remains discussed in this work where discovered in layers of the Kattendijk Formation (Lower Pliocene): Waaslandkanaal for NMB 42001, the holotype of the balaenid *Balaenella brachyrhynus*; Vrasenedok for RBINS M.2344, a partial cranium of *B. brachyrhynus*, and for RBINS M.1922, a partial cranium with a few postcranial remains of the monodontid *Casatia* sp.; and Verrebroekdok for a mysticete vertebra RBINS Vert-35044-02 associated to a lower tooth of the bluntnose sixgill shark *Hexanchus griseus* RBINS P.10797. Maps modified from Bisconti et al. (2017).

the Scheldt River, later renamed Vrasenedok (Nuyts 1990; Marquet 1995; Fig. 1), in Kallo.

The palynological analysis of a sediment sample associated with this cranium indicates the deposition and burial of this specimen in the Lower Pliocene Kattendijk Formation (5.0–4.4 Ma; De Schepper et al. 2009; see details above).

Description.—Ontogenetic stage: Many cranial sutures are partly to fully open: the parietal and supraoccipital can be manually separated from the frontals on the occipital shield, both the nasals and premaxillae are detached from the frontals, and only part of the right maxilla is attached to the corresponding frontal (Fig. 2), suggesting a relatively young individual. On the other hand, the supraoccipital-parietal sutures are closed, though with a visible suture line. Furthermore, all the preserved bones are thick (e.g., the nuchal crest made by the supraoccipital and parietals is 27 mm-thick anteromedially) and bone surfaces are made of compact bone, which are features of adults among modern balaenids (Buono et al. 2017). Together, these seemingly conflicting conditions point to either a late juvenile or young adult.

Cranial dimensions and size estimate: This neurocranium is unfortunately too fragmentary to document many cranial morphometrics. Still, some measurements can be compared to the holotype of *Balaenella brachyrhynus* (NMB 42001). The transverse width of the supraoccipital at a level 155 mm posterior to its anterior tip was originally greater than 264 mm, thus probably not much smaller than in NMB 42001 (330 mm). The minimum distance between the maxillae across the frontals in the interorbital region is estimated to be 55 mm, only slightly smaller than in NMB 42001 (63 mm). The length of the frontals on the vertex, taken from the anterior margin of the supraoccipital, is estimated to be 46 mm, somewhat smaller than in NMB 42001 (62 mm). These differences suggest an individual slightly smaller than NMB 42001. The body length of the latter, assumed to represent an adult (Bisconti 2005), has been estimated at about 5.3 m (Bisconti et al. 2021), so the individual represented by RBINS M.2344 was probably smaller than 5 m.

Maxilla: Only the posteromedial portion of the ascending process of the right maxilla is preserved. Its posterior outline is posteriorly convex in dorsal view, with a marked posteromedial corner (Fig. 2A$_3$, A$_4$). This process faces anteroposterolaterally and is moderately transversely convex in its preserved medial portion. A 21.5 mm-long and less than 22 mm-wide notch between the medial margin of the maxilla and the anterolateral margin of the frontal on the vertex most likely originally housed the narrow posterior part of the ascending process of the right premaxilla.

Frontal: The vertex and the proximal part of the two supraorbital processes is preserved. Though the left frontal is incomplete in this region, the joined frontals originally formed a trapezoid at the vertex in dorsal view, with the lateral margins converging anteromedially towards a transversely thick (about 30 mm) anterior margin (Fig. 2A$_3$, A$_4$). The dorsal surface of the frontals at the vertex is slightly anteroposteriorly and transversely convex, with a depressed medial region. The articular surface for the lateral part of the ascending process of the maxilla is visible on the right frontal (Fig. 2A$_1$, A$_2$), indicating that the posterior margin of the maxilla originally turned ventrolaterally and then posteroventrolaterally. A short and thin ridge is observed on the right frontal, 12.5 mm posterior to the posterior margin of the ascending process of the maxilla. It only extends for 40 mm posterolaterally, so it is much shorter than the frontal ridge described in *Morenocetus parvus* and *Eubalaena* spp. by Buono et al. (2017).

Somewhat better preserved on the left side (with no major transverse break, contra the right side), the proximal portion of the supraorbital process has a long axis that is directed posterolaterally and moderately ventrally (Fig. 2A$_1$–A$_4$). The anterodorsal surface of this region is transversely convex in its upper portion and slightly concave in its lower portion. No indication of the orbitotemporal crest could be found in that area.

Supraoccipital: The occipital shield reaches anteriorly to a level anterior to the supraorbital process, in line with the posterior margin of the ascending process of the maxilla.

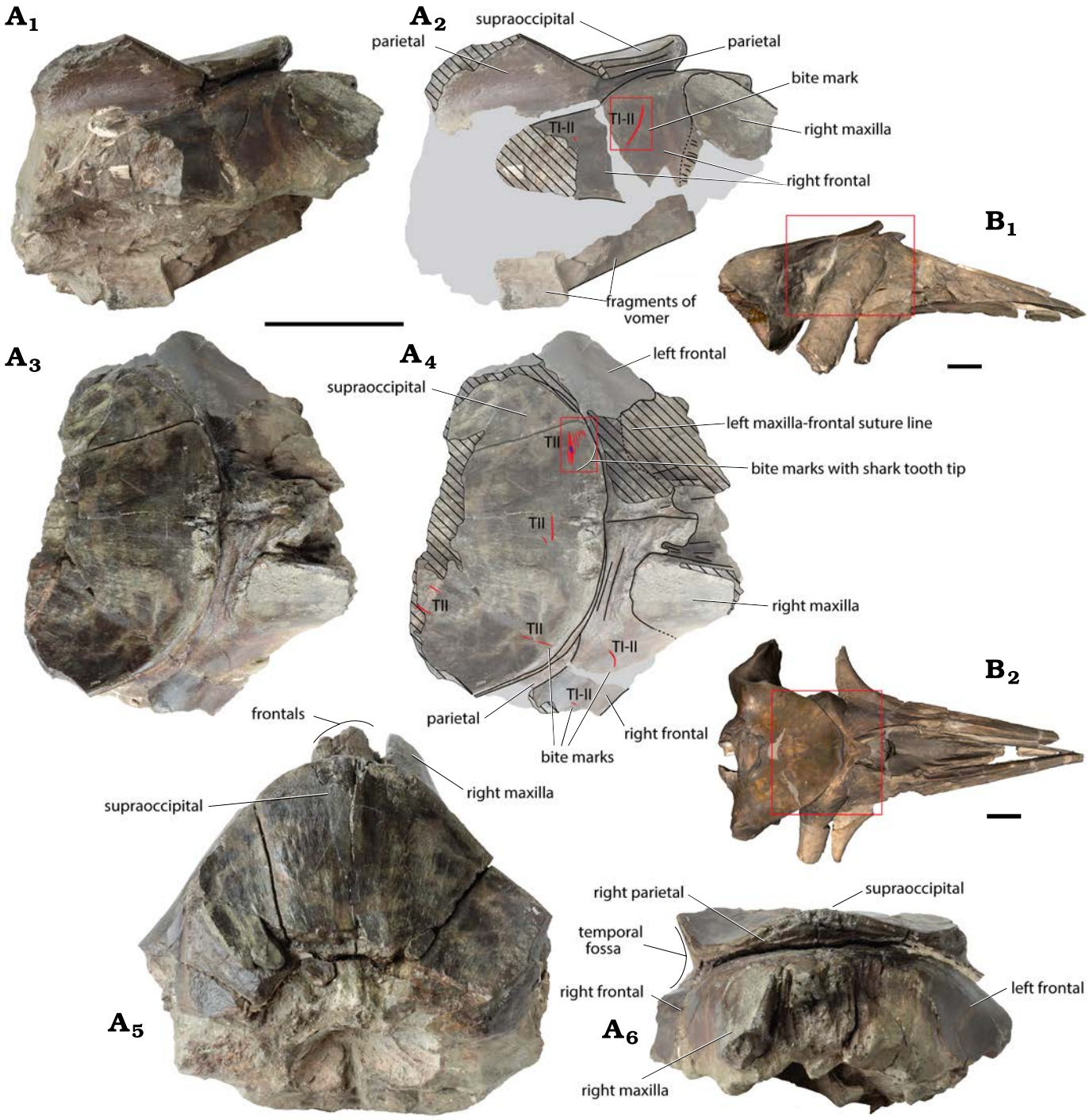

Fig. 2. Partial cranium of the balaenid *Balaenella brachyrhynus* Bisconti, 2005 **A**. RBINS M.2344 (Kattendijk Formation, Lower Pliocene; Vrasenedok, Belgium), right lateral view: photograph (A_1), explanatory line drawing (A_2), dorsal view: photograph (A_3), explanatory line drawing (A_4), posterodorsal (A_5) and anterior (A_6) views. **B**. NMB 42001 holotype (Kattendijk Formation, Lower Pliocene, Waaslandkanaal, Belgium), 3D model in right lateral (B_1) and dorsal (B_2) views provided for comparison. Grey shading indicates main parts covered with sediment; hatching, main break surfaces; red lines, shark bites marks; small blue spot, shark tooth tip interpreted as belonging to the bluntnose sixgill shark *Hexanchus griseus* (Bonnaterre, 1788); red rectangles in A, the location of detailed photos shown in Figure 3; red rectangles in B, the corresponding preserved part in RBINS M.2344. Bite mark types (TI–V) follow Collareta et al. (2017a). Scale bars 100 mm.

In dorsal view, the occipital shield has a rounded outline (Fig. $2A_3$, A_4). Its upper surface is subparallel to the dorsal surface of the frontals on the vertex for at least 175 mm. Most of the occipital shield thus slopes only weakly anterodorsally, with the exception of the anteromedial-most region, which rises more dorsally in relation to a thickening of the supraoccipital bone in that area (Fig. $2A_1$, A_2). The anterior portion of the shield's surface is thus transversely arched.

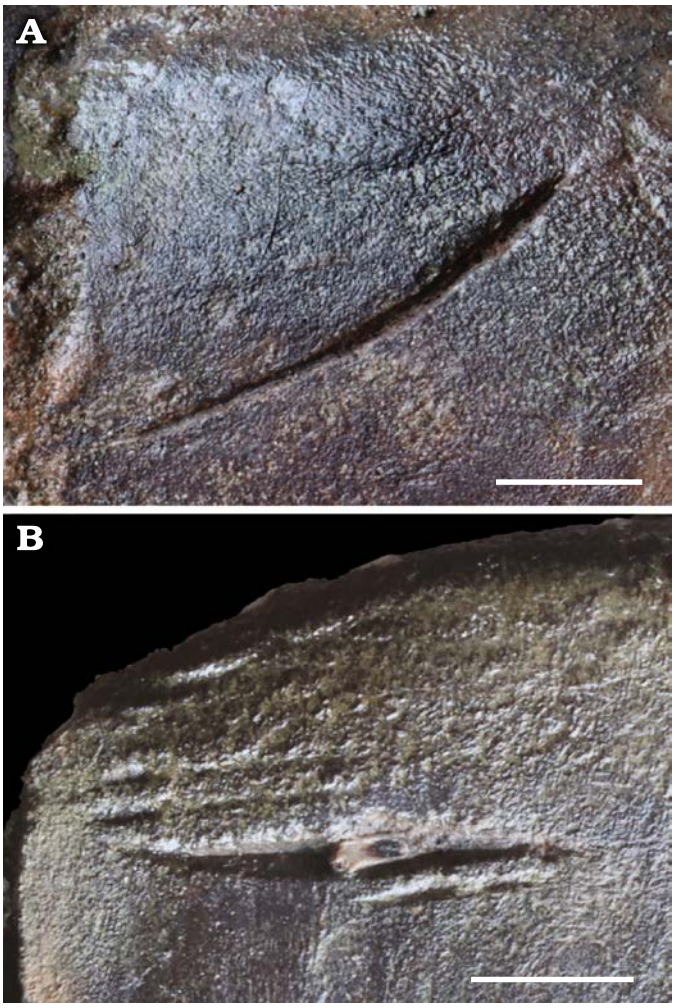

Fig. 3. Detail views of bite marks on the cranium of the balaenid *Balaenella brachyrhynus* Bisconti, 2005 (RBINS M.2344) from Kattendijk Formation, Lower Pliocene, Vrasenedok, Belgium. **A**. Long and deep TI or TII bite mark on the dorsolateral surface of the right frontal. **B**. Set of TII parallel bite marks on the anterior part of the occipital shield. The tip of a shark tooth, interpreted as belonging to the bluntnose sixgill shark *Hexanchus griseus* (Bonnaterre, 1788) is visible in the deepest and longest mark. Scale bars 10 mm.

Parietal: Dorsal to the proximal part of the supraorbital process, the parietal contributes as much as the supraoccipital (locally even slightly more) to the nuchal crest. This contribution decreases gradually towards the sagittal plane, together with the thickening of the supraoccipital (Fig. $2A_1$, A_2). In the preserved upper part of the right temporal fossa, the surface of the parietal is dorsoventrally concave and anteroposteriorly flat. Dorsal to the supraorbital process of the frontal, the parietal-frontal suture is directed posteroventrolaterally.

Remarks, comparison and identification.—In addition to its small size (see above), RBINS M.2344 shares with the holotype of *Balaenella brachyrhynus* a low slope of the anterior portion of the occipital shield (here at least 175 mm), which is subparallel to the dorsal surface of the frontals on the vertex (Fig. $2A_1$, A_2), a character proposed to be diagnostic for that species (Bisconti 2005). It further shares with the latter the anteromedially converging lateral margins of the frontals on the vertex, the thickening of the anteromedial edge of the occipital shield, and the posterolateroventrally directed supraorbital process. As it most likely originates from the same lithological unit (Kattendijk Formation) and locality (Kallo, NW Antwerp), we confidently assign RBINS M.2344 to the *B. brachyrhynus*. In view of its somewhat smaller dimensions and more open cranial sutures, it may represent an individual that was ontogenetically younger than the holotype.

Stratigraphic and geographic range.—Only found in the Kattendijk Formation, Zanclean (Lower Pliocene) of Belgium.

Suborder Odontoceti Flower, 1867
Infraorder Delphinida Muizon, 1984
Superfamily Delphinoidea Gray, 1821
Family Monodontidae Gray, 1821
Genus *Casatia* Bianucci, Pesci, Collareta, & Tinelli, 2019

Type species: *Casatia thermophila* Bianucci et al., 2019
Type locality: Arcille quarry, Campagnatico, Italy.
Age: Early Zanclean (Early Pliocene).

Casatia sp.

Figs. 4, 8.

Material.— RBINS M.1922, a partial cranium (Fig. 4A, C) with the associated atlas and axis, several detached vertebral epiphyses, and rib fragments (Fig. 4D). Vrasenedok, Kallo, NWW Antwerp (51°15'N, 04°14'E). Kattendijk Formation (about 6 m above the base), Lower Pliocene (Zanclean, 5.0–4.4 Ma) (Lambert and Gigase 2007; De Schepper et al. 2009).

Description.—*Ontogenetic stage*: Lambert and Gigase (2007) indicated that the individual represented by RBINS M.1922 was not fully mature, due to the four unfused vertebral epiphyses (from unknown regions of the column) found associated with the cranium. The posterior epiphysis of the axis is fully ankylosed, with no suture line visible, but such a fusion occurs very early in the phocoenid *Phocoena phocoena* (Galatius and Kinze 2003; see also Moran et al. 2015). Furthermore, all the preserved cranial sutures of RBINS M.1922 are either open or only partly closed. Among those, the basisphenoid-presphenoid suture (or intersphenoidal synchondrosis) is fully open, while it closes near the time of cranial maturity in the delphinid *Tursiops truncatus* (Mead and Fordyce 2009). We can therefore confirm a juvenile stage for this individual.

Estimated body length: Lambert and Gigase (2007) found that the cranium of RBINS M.1922 is smaller than in adults of the monodontid *Delphinapterus leucas*.

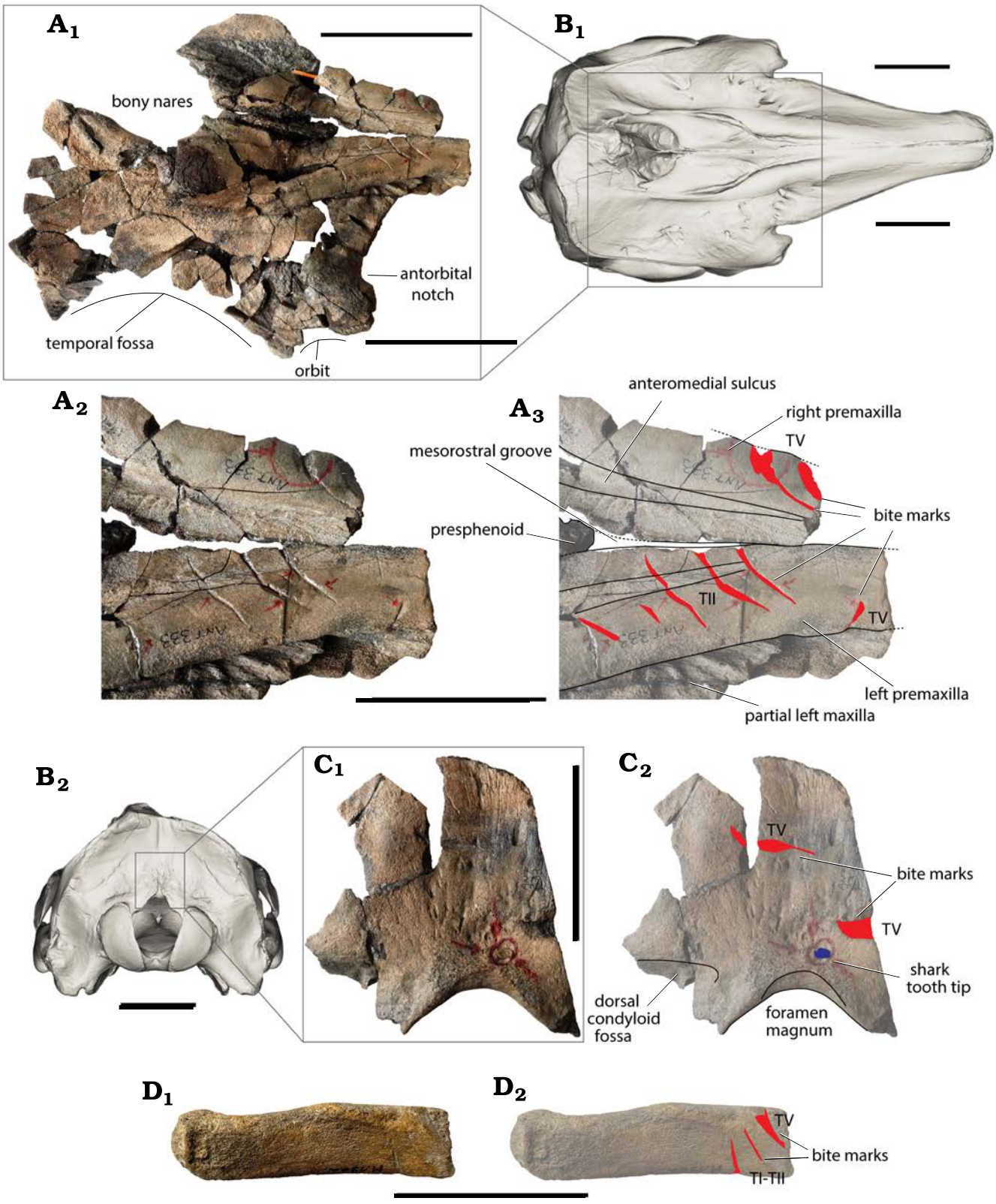

Fig. 4. **A**, **C**, **D**. Monodontid *Casatia* sp. (RBINS M.1922) from Kattendijk Formation, Lower Pliocene, Vrasenedok, Belgium. **A**. Partial cranium in dorsal view (A_1), detail of the rostrum base in dorsal view: photograph (A_2), explanatory line drawing (A_3). **C**. Fragment of the occipital shield in posterior view: photograph (C_1), explanatory drawing (C_2). **D**. Proximal part of a single-headed rib in lateral view: photograph (D_1), explanatory drawing (D_2). **B**. 3D model of the cranium of the Recent beluga *Delphinapterus leucas* Pallas, 1776 (USNM 305071) in dorsal (B_1) and posterior (B_2) views; to indicate the position of the preserved parts (model downloaded from Phenome10k). Red lines, shark bites marks; small blue spot, shark tooth tip interpreted as belonging to the extinct lamnid shark *Carcharodon plicatilis* (Agassiz, 1843). Bite mark types (TI–V) follow Collareta et al. (2017a). Scale bars A_1, B, 100 mm; A_2, A_3, C, D, 50 mm.

Therefore, the body length was most likely less than 3.5 m (see Brodie 1989).

Remarks.—Because of its fragmentary state, this specimen was originally identified as Monodontidae indet. (Lambert and Gigase 2007). Following this publication, several other monodontids were described and named from the Pliocene of the east coast of North America, Japan, and the Mediterranean (Vélez-Juarbe and Pyenson 2012; Ichishima et al. 2019; Bianucci et al. 2019; Merella et al. 2022b), prompting the reevaluation of the systematic affinities of the southern North Sea specimen. RBINS M.1922 shares with *Casatia thermophila*, from the Lower Pliocene of Italy, the presence of a median depression anterior to the premaxillary sac fossae, formed by the depressed medial part of the two premaxillae, and the medial part of the premaxilla-maxilla suture not paralleling the anterolateral profile of the external bony nares, but rather diverging posterolaterally.

The only difference noted by Bianucci et al. (2019) is the greater elevation of the presphenoid in the area anterior to the nares in RBINS M.1922. However, the condition in that specimen may be at least partly due to inaccuracies during the reconstruction of this region. Merella et al. (2022b) proposed another difference, with the antorbital notch of *C. thermophila* being deeply medially excavated. However, the medial margin of the antorbital notch is not preserved in RBINS M.1922 (Fig. 4A), preventing such a comparison. In the interpretive line drawing of the cranium of RBINS M.1922, the right premaxilla is reconstructed as somewhat longer posteriorly compared to the holotype of *C. thermophila*. However, here again this region is not adequately preserved to allow for a reliable comparison. The ventral view of the axis of M.1922 (Lambert and Gigase 2007: fig. 6a) is somewhat different from the condition in the referred specimen of *C. thermophila* (Merella et al. 2022b): the former displays a longer articulation surface for the hypapophysis of the atlas.

Though only a few measurements could be taken on the material of *Casatia thermophila*, cranial and axis dimensions are roughly similar with RBINS M.1922. As a sister-group relationship has been determined by Bianucci et al. (2019), and pending the discovery of more complete monodontid remains from the Early Pliocene of the North Sea and the Mediterranean, we identify RBINS M.1922 as *Casatia* sp.

Shark bite marks and tooth fragments embedded in bone

Balaenella brachyrhynus Bisconti, 2005 (RBINS M.2344)

Shark bite marks.—This partial neurocranium displays bite marks in the dorsal and lateral regions (Figs. $2A_1$–A_4, 3). As ventral elements are either missing or poorly preserved, the presence of bite marks could not be assessed there. On the occipital shield, a first set of marks is located anterodorsolaterally, on the left side (Figs. $2A_3$, A_4, 3B). It includes a series of seven subparallel, approximately transversely directed TII marks (simple and superficial grooves; see Cigala-Fulgosi 1990) with lengths of 12, 28.5, 18, 17, 9, 6, and 7 mm, from posterior to anterior. The maximum distance between the first mark and the last mark taken perpendicular to their long axis is 17 mm. The second mark, which is the longest and by far the deepest and broadest, contains the tip of a shark tooth's cusp (see below) and displays a more irregular anterior margin with a distinct broadening at the level of the tip of the tooth.

More medially on the occipital shield, a second set includes two TII marks: the longer one (20 mm) is slightly curved and transversely directed, and the shortest (8 mm) is similarly slightly curved and obliquely directed. Along the right anterolateral margin of the shield, a 34 mm-long, rectilinear TII mark is directed roughly anteroposteriorly. A last set of two, probably TII incomplete oblique and subparallel marks, 18 mm apart from each other, is located along the broken posterior margin of the shield on its right side.

The anterodorsal lateral surface of the proximal portion of the right supraorbital process of the frontal displays two marks (Fig. $2A_3$–A_4). The longest (39 mm) is also the deepest; it is moderately curved with its deepest part being transversely directed and the shallowest part being obliquely directed (detail in Fig. 3A). The shortest mark (4.5 mm) is obliquely directed. Both are interpreted as either TI or TII marks (both types correspond to simple grooves, but produced with different movements of the tooth edge, either with a cutting direction roughly perpendicular to the intersection of the plane of movement of the tooth and of the plane of the bone surface, for TI, or parallel to this intersection, for TII; Cigala-Fulgosi 1990).

All marks are preserved in thick and compact bone. None of the marks show indications of healing (bone overgrowth/callus formation).

Shark tooth fragment embedded in bone.—The tooth fragment embedded in the supraoccipital has an apicobasal length (i.e., height) of 6.28 mm, a maximum mesiodistal length (i.e., width) of 1.94 mm, and a maximum labiolingual length (i.e., thickness) of 1.35 mm (Fig. 5). The oblique break surface has a maximum diameter of 5.21 mm, with a large portion (about 2.7 mm) being made of the sole enameloid layer. In mesial/distal view (i.e., side or profile view) the preserved labial and lingual outlines are slightly convex, similar to the longest cutting edge in labial/lingual view. The preserved portions of the cutting edges form an angle of about 45°. The resolution of the 3D model does not allow for the assessment of the presence/absence of serrations along cutting edges.

Interpretation.—Among all the bite marks detected on this neurocranium, the set of seven parallel marks on the supraoccipital associated with the shark tooth fragment is potentially the most informative. Such a combination of linear

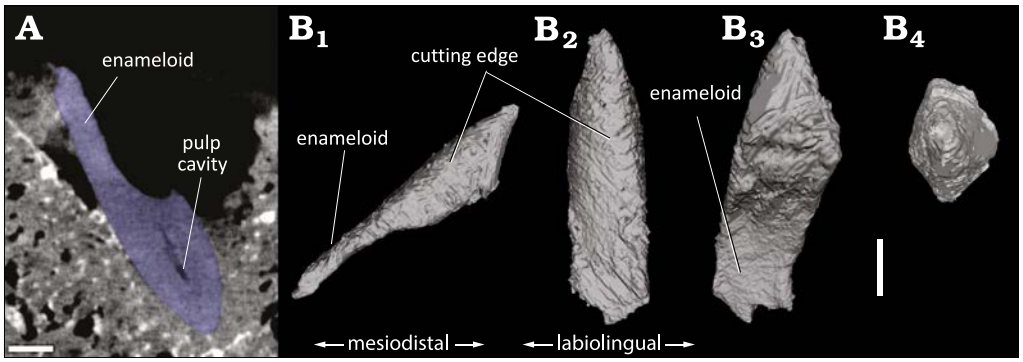

Fig. 5. 3D model of the tip of shark tooth found embedded in the occipital shield of the balaenid *Balaenella brachyrhynus* Bisconti, 2005 BINS M.2344) (Kattendijk Formation, Lower Pliocene, Vrasenedok, Belgium), reconstructed from a micro-CT scan of the bone fragment. The tooth is interpreted as belonging to the bluntnose sixgill shark *Hexanchus griseus* (Bonnaterre, 1788). **A**. Micro-CT slice showing a section of the tooth tip (blue) in the cetacean bone. **B**. 3D model in labial or lingual (B_1), profile (mesial) (B_2), proximal (B_3), and apical (B_4) views. Scale bar 1 mm.

marks close to each other is reminiscent of marks produced by the lower teeth of hexanchid sharks (e.g., Merella et al. 2021, 2022a). Therefore, several teeth of *Hexanchus* sp. from the Neogene of Antwerp were brought close to the bite marks to test for a match in the spacing of the marks. A particularly good match was found with the (first) lower tooth of *H. gigas* RBINS P.968 (now considered to represent a junior synonym of *H. griseus*; see Cappetta 2006), figured by Leriche (1926: pl. 29) and Nolf (1988: pl. 51), with a mesiodistal length of 45 mm and eight distal cusplets. A possible sequence of events is as follows (Fig. 6): I—contact of the principal cusp and at least five distal cusplets with the supraoccipital bone of the whale, followed by a movement of the shark's jaws towards the right side of the whale cranium, with the shark tooth's mesiodistal axis being oblique relative to the direction of the movement, II—break of the tip of the principal cusp after 14 mm of contact, with the tip remaining stuck in the compact bone and a local broadening of the main bite mark, and III—from this level, only the truncated principal cusp retains a contact with the bone, together with the more mesial part of the tooth crown (either mesial serrations or even the mesial-most portion of the truncated principal cusp), creating an additional mark located posterior to the mark made by the main cusp.

The size and proportions of the embedded tooth fragment obtained from the micro-CT imaging agree with the size and proportions of the principal cusp for hexanchid lower teeth (e.g., Jambura et al. 2020, including the extent of the pulp cavity; OL and FM personal observations on *Hexanchus* sp. teeth from the Neogene of Antwerp). The only hexanchid known from the Kattendijk Formation is *Hexanchus griseus* (previously divided in two species, *H. griseus* and *H. gigas*; Leriche 1926; Herman 1975), a species that has been reported from the locality of the Vrasenedok by dozens of individual teeth (in 't Hout 1985). Interestingly, a large lower tooth of *H. griseus* (RBINS P.10797) found associated with a mysticete vertebra (RBINS Vert-35044-02) in the Kattendijk Formation at the nearby locality of the Verrebroekdok (Kallo, Antwerp; collected by LDC), displays a principal cusp with a broken tip that appears to have happened prior to fossilisation (Fig. 7).

The diet of larger individuals of the extant bluntnose sixgill shark *Hexanchus griseus* includes marine mammals of various sizes, and this shark has been reported as actively preying upon pinnipeds and dolphins, as well as scavenging on larger cetacean carcasses (Ebert 1994; Heithaus 2001; Assemat et al. 2024). From an evolutionary viewpoint, the increase in size noted for *Hexanchus* spp. during the late Paleogene and Neogene has been correlated with a shift to a marine mammal-dominated diet (Adnet and Martin 2007). However, though hexanchiform shark teeth were found associated to marine tetrapod remains as early as the Jurassic (Bogan et al. 2016; Serafini et al. 2024), direct evidence of past trophic relationships between *Hexanchus* and marine mammals remains extremely scarce, with only one record of bite marks on sirenian bones from the Pliocene of Italy attributed to *H. griseus* (Merella et al. 2021, 2022a), in addition to the description of *H. griseus* teeth from a whale fall assemblage from the Early Pleistocene of Italy (Baldanza et al. 2025).

Among other sharks identified from the Kattendijk Formation (Herman 1975; in 't Hout 1985; Bor and Peters 2015), with the exception of *Isistius* sp. (= cookie cutter shark) whose superficial bites would not reach bone, only *Somniosus microcephalus* (Greenland shark), *Carcharodon plicatilis* (= *Carcharodon hastalis*, broad form), *Carcharodon carcharias* (great white shark), and especially large species of *Carcharhinus* (e.g., bull shark *C. leucas*, oceanic white tip shark *C. longimanus and* dusky shark *C. obscurus*, whose teeth are much larger compared to the ones from the Belgian Mio-Pliocene) have previously been proposed to feed on marine mammals, at least occasionally and either via scavenging or active predation (Heithaus 2001; Bianucci et al. 2010; MacNeil et al. 2012; Nielsen et al. 2019; Godfrey et al. 2025). None of these taxa's teeth match the shape of the tooth tip embedded in the whale bone. Furthermore, their bites could not have produced the set of parallel marks described here. We therefore identify the author of this bite as a large individual of *Hexanchus griseus*.

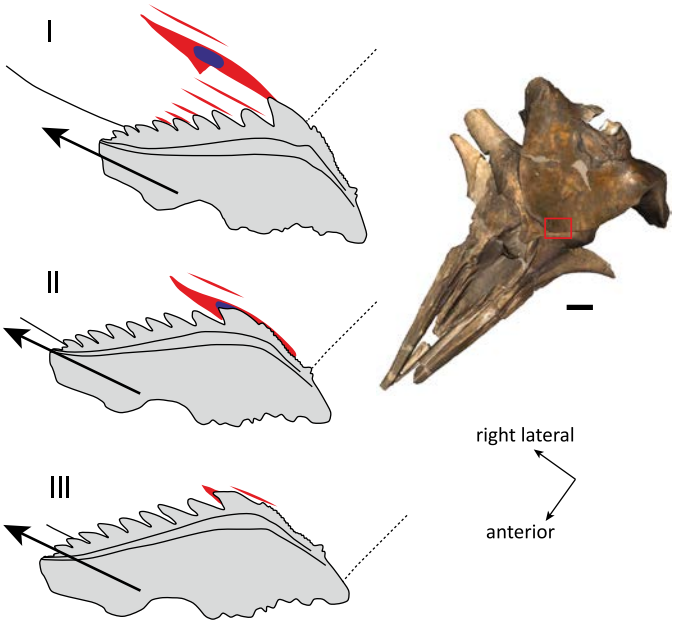

Fig. 6. Reconstructed bite sequence corresponding to the set of parallel bite marks observed on the occipital shield of the balaenid *Balaenella brachyrhynus* Bisconti, 2005 (RBINS M.2344). The shark tooth best matching the bite marks is the large (first) lower tooth of the bluntnose sixgill shark *Hexanchus griseus* (Bonnaterre, 1788) (RBINS P.968, the Neogene of Antwerp). The proposed sequence includes: (I) contact of the principal cusp and at least five distal cusplets with the supraoccipital bone, followed by a movement of the shark's jaws towards the right side of the whale cranium and at an angle with the tooth's mesiodistal axis, (II) break of the tip of the principal cusp, with the tip remaining stuck in compact bone and related local broadening of the main bite mark, and (III) only the truncated principal cusp retains a contact with the bone, together with the more mesial part of the tooth crown, creating an additional mark posterior to the mark made by the principal cusp. The cranium of the holotype of *B. brachyrhynus* (NMB 42001) is shown in the same orientation to illustrate the position of the bite marks (red rectangle) and the direction of the bite. Large arrows, the proposed direction for the movement of the shark tooth; small arrows, the orientation of the whale cranium; red lines, shark bite marks; blue spot, broken shark tooth tip embedded in whale bone. Scale bar for the cranium 100 mm; interpretive drawings not to scale.

The set of subparallel TII bite marks located on the dorsal surface of the cranium of the whale much better matches hexanchid teeth from the lower jaw that have a multi-cuspid tooth-design that is well adapted to cut through flesh (i.e., cutting-type) by shaking the head (= head thrashing). The upper teeth of hexanchids are smaller, narrower, with a lower number of cusplets or even devoid of cusplets in para-symphyseal tooth positions (i.e., grasping type, sensu Cappetta 1986: fig. 8b). Consequently, it is likely that either the shark or the whale was not in its natural position (belly down) at the moment of the bite. In the first hypothesis, the shark hit the whale upside down, while the shark was rolling onto its back, a behaviour called inverted feeding, as observed in several other shark species feeding on whale carcasses (e.g., Tucker et al. 2019: fig. 1b, c). In the second hypothesis, the whale's body was not in its natural position, but rather upside down, with the shark biting in a horizontal, natural position (see McNeil et al. 2016 for a description of the feeding behaviour of extant *Hexanchus griseus*). Such a position of the whale could indicate an interaction between a shark and a floating carcass. Modern balaenids are known to be positively buoyant (Nowacek et al. 2001), and though *Balaenella brachyrhynus* is a much smaller whale, the carcass of an individual of this Early Pliocene species may have floated for some time at the sea surface, either because it was initially positively buoyant or because of the accumulation of decomposition gases while the carcass was lying on the seafloor at shallow depth (Moore et al. 2020). Although extant bluntnose sixgill sharks are best known for their bottom dwelling behaviour, and documented for scavenging on carcasses and bait near the sea floor (e.g., McNeil et al. 2016), *H. griseus* is also known for migrating from deeper to shallower waters during the night, and descending during the day, which is most likely related to foraging behaviour, and supported by observation of sixgills surfacing in response to recent human fishing operations (Andrews et al. 2009; Ebert and Stehmann 2013; Coffey et al. 2020).

Individuals of the extant *H. griseus* can reach total lengths up to at least 4.82 m and probably to about 5.5 m (Ebert and Stemann 2013), with a documented mouth width and mouth length of 700 mm and 380 mm, respectively in a 3.9 m-long female (Mili et al. 2021). It is clear that an adult *H. griseus* can thus produce very large gapes, even though their capability to protrude the upper jaws has not been documented during feeding (Wilga 2002; McNeil et al. 2016). A large specimen of *H. griseus*, possibly more than 4 m-long, would thus most likely be able to produce a gape that is large enough to engulf the posterior part of the head of a (drifting) young *B. brachyrhynus* individual, whose dorsoventral diameter likely did not exceed 550 mm.

The action of scavengers may then have led to the dismemberment of the carcass and the deposition of separate elements on the seafloor preceding burial. The set of parallel marks on the occipital shield are the only ones on this neurocranium that allow for a tentative determination of the shark that performed the bite. For most of the other marks, it is only possible to exclude shark species with serrated teeth (e.g., *Carcharocles* [= *Otodus*] *megalodon* or *Carcharodon carcharias*, of which only the latter is present in the Kattendijk Formation, albeit rare and only confirmed from the mid and higher parts of its sequence), and none of these marks displays a pattern that would unambiguously indicate a second bite by *H. griseus*. We cannot rule out the hypothesis that some of these marks, especially the deepest and longest one, located on the dorsolateral surface of the right frontal of the whale (Fig. 3A), may have resulted from a powerful bite by another large shark species with single-cusped teeth, for example *Carcharodon plicatilis* (see below). Extant whale carcasses are often scavenged upon by multiple shark species, either simultaneously, or at a different times and places in the water column, whether drifting at the surface or while sinking to the sea floor.

Finally, it should be noted that analogue sets of sub-

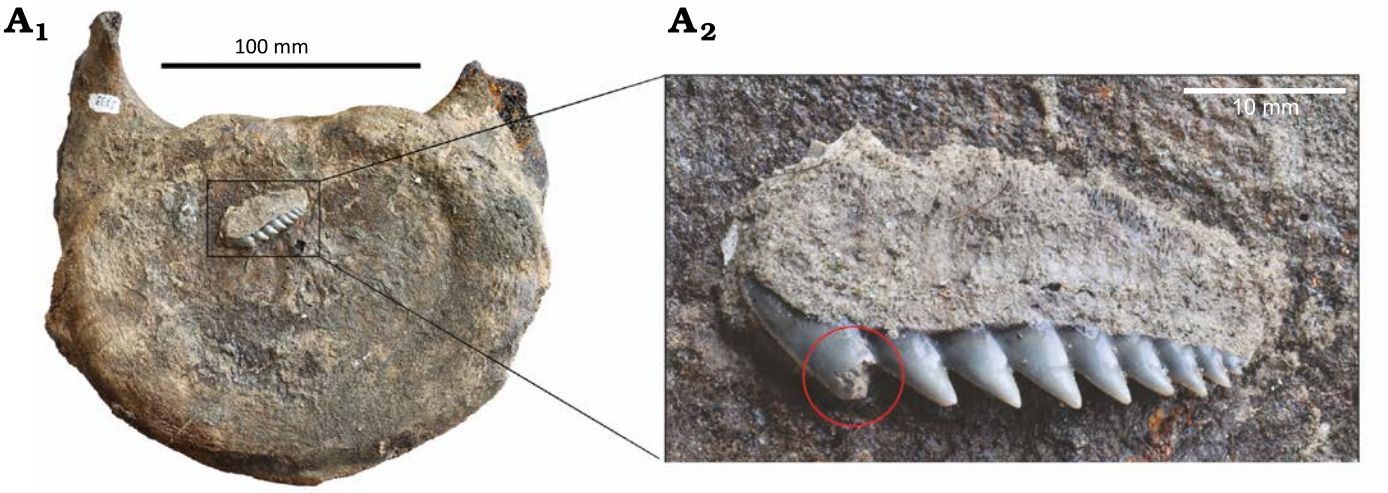

Fig. 7. Vertebra (probably 7th cervical) of a mysticete Balaenopteridae indet. (RBINS Vert-35044-02) from Kattendijk Formation, Lower Pliocene, Verrebroekdok, Belgium; in posterior view (A_1), associated with a large lower tooth of the bluntnose sixgill shark *Hexanchus griseus* (Bonnaterre, 1788) (RBINS P.10797) (A_2). Note the broken apex of the principal cusp on the shark tooth (red circle).

parallel TII bite marks, but narrower and with smaller inter-mark spacing, have been observed on early Holocene bones of the common bottlenose dolphin *Tursiops truncatus* from the North Sea; these were interpreted as possibly resulting from scavenging by rays (van Netten and Reumer 2009). In view of modern dietary preferences of extant batoids (Ebert and Stehmann 2013), i.e., feeding on invertebrates and demersal fishes (not on marine mammals), other hypotheses might instead be preferable, such as scavenging by sharks.

Casatia sp. RBINS M.1922

Shark bite marks.—As briefly described in Lambert and Gigase (2007), the main set of bite marks on this partial cranium is located on the dorsal surface of the rostrum base. The right premaxilla displays a series of five oblique, somewhat sinuous, and subparallel marks, with the deepest and broadest part being located medially (Fig. 4C). The distance between the lateral tip of the first mark and the lateral tip of the last mark is 51 mm. The two posteriormost marks are the shortest (12 and 8 mm) and shallowest, followed by somewhat longer marks with lengths of 29, 28.5, and 24.5 mm. These five marks are interpreted as TII marks, resulting from a single bite. A shorter (8 mm) TV mark (corresponding to the removal of a wedge-shaped chip of bone; see Collareta et al. 2017a) is also seen on the right premaxilla, anterior and perpendicular to this series.

The left premaxilla displays two deep TV marks, with the main cut surface parallel to the other mark, facing anterodorsolaterally. The posteriormost mark has a length of 25 mm, with a maximum width of the main cut surface of 4.2 mm. The shallower medial part of this mark has the same direction as the shallowest lateral part of the five marks on the right premaxilla. More fragmentarily preserved, the anteriormost mark on the left premaxilla has a length of 13.5 mm and a maximum width of the main cut surface of 4.9 mm.

On the occipital shield, two additional TV marks are partly preserved, both oblique and subparallel, with the main cut surface facing posterodorsally (Fig. 4C). The mark that is higher on the shield is 24 mm long, with a maximum width of the main cut surface of 2.7 mm. The second mark is preserved over a distance of 9.6 mm, with a maximum width of the main cut surface estimated at 5.6 mm (surface somewhat damaged). Six millimetres medioventrally to this second mark, the tip of a shark tooth (see below) is deeply embedded in the bone, directed anterolaterodorsally and without any related bite mark representing a cutting movement, therefore merely corresponding to a direct impact on the bone surface.

Three bite marks are preserved on the lateral surface of the proximal portion of a single-headed rib (Fig. 4D): two slightly diverging, transversely to more obliquely directed TI-TII marks, the proximal one being 8.3 mm long and the distal one being 6.6 mm long, and an oblique TV mark being 12.4 mm long with a maximum width of the main cut surface of 4.6 mm. The latter deeply cuts into the rib and may be responsible for the presumably post-mortem break of the distal portion of the bone.

As for *Balaenella brachyrhynus* RBINS M.2344, most of the bite marks are preserved on compact bone (namely the porcelanous part of the premaxillae and the occipital shield) and there is no indication of bone healing for any of the marks.

Shark tooth fragment.—The shark tooth fragment embedded in the occipital shield of *Casatia* sp. (RBINS M.1922) has an apicobasal length (i.e., height) of 4.65 mm, a maximum mesiodistal length (i.e., width) of 3.83 mm, and a maximum labiolingual length (i.e., thickness) of 1.75 mm (Fig. 8). The oblique break surface has a maximum diameter of 3.54 mm. In the basal part of the fragment, only the enameloid layer

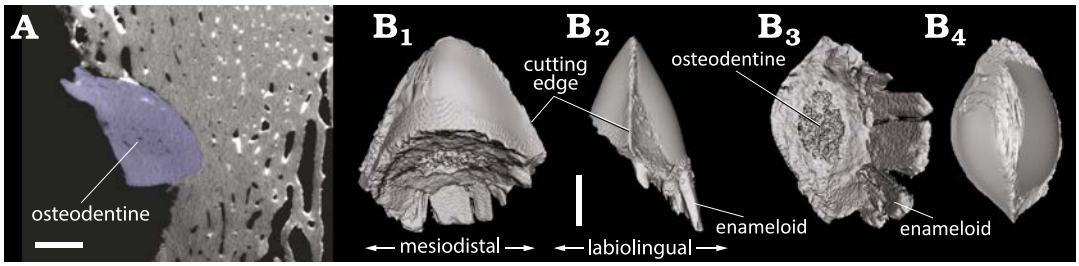

Fig. 8. 3D model of the tip of shark tooth found embedded in the occipital shield of the monodontid *Casatia* sp. (RBINS M.1922) from Kattendijk Formation, Lower Pliocene, Vrasenedok, Belgium, reconstructed from a micro-CT scan of the bone fragment. The tooth is interpreted as belonging to the extinct lamnid shark *Carcharodon plicatilis* (Agassiz, 1843). **A**. Micro-CT slice showing a section of the tooth tip (blue) in the cetacean bone. **B**. 3D model in labial or lingual (B_1), profile (mesial) (B_2), proximal (B_3), and apical (B_4) views. Scale bars 1 mm.

is preserved for 1.39 mm. In mesial/distal view, the labial and lingual outlines are markedly convex and symmetrical. In labial/lingual view, the outline of the tooth tip is broadly rounded, much less pointed than in the *Hexanchus* sp. tooth tip associated to *Balaenella brachyrhynus* (RBINS M.2344). The tooth's mesial and distal cutting edges are roughly symmetrical and form an angle of 55°. No serrations could be detected along the best-reconstructed parts of the cutting edges (especially the ones preserved just outside the cetacean bone). In proximal view, a spongier central region is distinct, most likely corresponding to osteodentine.

Interpretation.—All morphological features and proportions of the shark tooth tip embedded in the occipital region (biconvex cross section, symmetry, absence of serrations on cutting edges, and presence of osteodentine that is not encased by orthodentine) match perfectly large teeth of the lamnid shark *Carcharodon*, and more specifically *C. plicatilis* (OL and FM personal observations on teeth from the Neogene of Antwerp; Godfrey et al. 2025). In contrast to *C. carcharias* (whose teeth have serrated cutting edges), *C. plicatilis* is more frequently recorded in the Kattendijk Formation (Herman 1975; in 't Hout 1985; Bor and Peters 2015). The other sharks from this unit thought to feed at least occasionally on marine mammals (see above), namely *Hexanchus griseus* and *Somniosus microcephalus*, have pseudoosteodont teeth that include a layer of orthodentine (Jambura et al. 2020) and their teeth are very differently shaped (see above for *H. griseus*, and much more slender and asymmetrical in *S. microcephalus*). Two other possible candidates with large teeth, the extinct otodontid *Carcharocles megalodon* and *Isurus* cf. *oxyrinchus* (longfin mako shark) (e.g., Cigala-Fulgosi 1990; Ehret et al. 2009; Collareta et al. 2017a; Mucientes et al. 2025), are not recorded in the Kattendijk Formation (Herman 1975; in 't Hout 1985), and the former species has distinctly serrated teeth that depart from the condition in the shark tooth tip studied here. Therefore, we propose that by far the most likely candidate for this bite is *C. plicatilis*.

If this bite was made on a living whale or on a complete, floating carcass, the shark's teeth had to pierce a thick layer of neck muscles (about 10 cm if similar to modern monodontids) before contacting the occipital shield just above the foramen magnum, thus suggesting a powerful bite from a relatively large *C. plicatilis* individual. The recent study of stomach contents for another large lamnid, the extant shortfin mako *Isurus oxyrinchus* revealed complete dolphin heads, separated from the rest of the body (Mucientes et al. 2025). This indicates that these large sharks at least occasionally sever the head of dolphins by a powerful bite along the neck (see also Arnold 1972; Di Beneditto 2004), while in other cases, smaller dolphins may be cut at a different level of the body before being swallowed (e.g., Arnold 1972; Monteiro et al. 2006). The absence of digestion marks on the preserved bones of *Casatia* sp. (RBINS M.1922) suggests that the head of this monodontid was not swallowed by the shark after the bite along the neck, possibly because it was too large.

The most informative set of bite marks is the one on the dorsal surface of the two premaxillae. It can be proposed that a powerful single oblique bite, along an axis from the left posterior side of the rostrum base to the right anterior side, produced most of the marks detected in that region (except for the shorter mark located anteriorly on the right premaxilla). Such a bite implies that the snout of the whale entered at least partly in the mouth of the shark, a process that would have been facilitated if the whale was still alive or floating as a carcass (as opposed to a carcass lying on the seafloor). As these marks lack any indication of serration (which is especially informative for the TV marks on the left premaxilla), they do not contradict the identification of the tooth fragment from the occipital region as belonging to *Carcharodon plicatilis*. Interestingly, in odontocetes the region of the head just above the rostrum base is occupied by the fat-rich melon (e.g., McKenna et al. 2012). The latter is especially voluminous in the extant monodontids *Delphinapterus leucas* and *Monodon monoceros* (e.g., Richard et al. 2024). It can be reasonably hypothesized that it was also the case in their Early Pliocene relative, making this region particularly attractive for a predator or scavenger. A similar interpretation was proposed for the fat-rich spermaceti organ of extinct sperm whales, preferentially targeted by sharks (Benites-Palomino et al. 2022).

Concluding remarks

In this work, two cetacean specimens from the Lower Pliocene Kattendijk Formation (Zanclean, 5.0–4.4 Ma) in the Port of Antwerp (Belgium, southern North Sea) were analyzed with a focus on shark bite marks. In addition, shark tooth fragments embedded in cranial bones were investigated via micro-CT imaging.

The newly acquired partial cranium of a subadult to young adult balaenid is identified as belonging to the diminutive species *Balaenella brachyrhynus*, with a body length probably lower than 5 m. Located on the occipital shield, the main set of bite marks found on this specimen is associated with a shark tooth fragment. All the features of the bite mark and tooth fragment point to the hexanchid *Hexanchus griseus* as responsible for this bite. Among the other bite marks, a long and deep mark on the frontal may indicate a powerful bite by the large lamnid *Carcharodon plicatilis*.

The second studied specimen, the partial skeleton of a juvenile individual (body length less than 3.5 m) of a monodontid toothed whale, previously referred to Monodontidae indet. (Lambert and Gigase 2007), is here more precisely attributed to *Casatia* sp. A shark tooth fragment found deep in the occipital region of the cetacean is attributed to *Carcharodon plicatilis* and the related bite is tentatively proposed to correspond to an attempt to separate the head from the rest of the body, a behaviour that is recorded in several large modern sharks. Several other bite marks on the monodontid cranium do not contradict the identification of the author of the bites as *C. plicatilis*, and one series of bite marks corresponds to a powerful bite in the melon area of the whale's head, a region that is especially rich in fat tissues.

In both cases, it remains difficult to distinguish between scavenging and active predation. For the *Balaenella brachyrhynus* specimen, the main *H. griseus* bite may have occurred with the whale's body upside down, thus suggesting scavenging on a carcass that was floating on the surface (or in neutral buoyancy in the water column), although inverted feeding by the shark on a whale in natural position remains an alternative viable interpretation. For the monodontid, active predation by a large *C. plicatilis* specimen is a reasonable hypothesis, supporting the idea that the lack of serrations on teeth, as seen in *C. plicatilis*, and contrasting for example with its extant close relative the great white shark *Carcharodon carcharias*, did not preclude active predation on medium-size marine mammals (e.g., Bianucci et al. 2010). The two studied whale specimens can be considered as attractive prey items, considering the amount of fat-rich tissue and the relatively slow swimming style in modern balaenids and monodontids (Würsig et al. 2018).

Trophic interactions between sharks and relatives of *B. brachyrhynus* and *Casatia* sp. are rare in the fossil record. Existing examples are the holotype skeleton of the larger balaenid *Antwerpibalaena liberatlas*, from the upper Pliocene of the Port of Antwerp, which displays shark bite marks (not analyzed in detail in the original work; Duboys de Lavigerie et al. 2020); whale forelimb bones from the Pliocene of Italy also show bite marks and may belong to a balaenid (Terranova et al. 2025); and isolated bones of the beluga *Delphinapterus leucas* (recovered as a close relative of *Casatia* in a recent phylogenetic analysis; Bianucci et al. 2019) from the late Pleistocene of the southern North Sea occasionally display bite marks (Post 1999; Klaas Post, personal communication 2025).

Today, the geographic distribution of the two modern monodontid species, *D. leucas* and the narwhal *Monodon monoceros*, is restricted to cooler waters from the Arctic to subarctic regions (Würsig et al. 2018). Small-sized balaenids went extinct during the late Pliocene (Marx and Lambert 2021; Bisconti et al. 2021) and giant balaenids in the genera *Balaena* and *Eubalaena* are not regular visitors of the southern North Sea (van der Meij and Camphuijsen 2006; Haelters et al. 2018 and references therein). The shift of monodontids and of the bowhead *Balaena mysticetus* to cooler regions reduces the risk of attacks (and scavenging) by large sharks with a more temperate to warm-water distribution. Only the Greenland shark *Somniosus microcephalus* is known to feed on dead or moribund *M. monoceros* (Beck and Mansfield 1969), and no predation or scavenging by sharks has been reported for *Balaena mysticetus* (Breed 2021). Meanwhile, younger individuals of other balaenid species with a more temperate distribution are at risk of predation by large sharks (e.g., *Carcharodon carcharias* on young individuals of the North Atlantic right whale *Eubalaena glacialis*; Taylor et al. 2013).

Several of the shark species recorded in the Kattendijk Formation (Zanclean, 5.0–4.4 Ma) that are known to prey upon cetaceans have survived until modern times, including *C. carcharias*, *H. griseus* and *S. microcephalus*. However, it is striking that none of them are common visitors of the southern North Sea in the present time (Ebert and Stehmann 2013).

At present, the bluntnose sixgill shark *H. griseus* is completely absent in the southern North Sea, although it is one of the most common and wide-ranging extant shark species. This includes occurrences in European waters from southern Spain up to northern Norway, preferring deepwater demersal and pelagic environments of the continental and insular shelves and slopes. In general, this is also the case for the Greenland shark *S. microcephalus* that has somewhat similar habitat preferences, but with a distribution that extends further north into arctic waters, and with very few individual records in the southern North Sea (Poll 1947; Nijssen and De Groot 1980; Rappé and Eneman 1988). In contrast, the extant great white shark *C. carcharias* prefers warmer to temperate waters, where it has a circumglobal distribution with its northeastern Atlantic limits off Brittany (northwestern France). Though other parameters, like changes in habitat conditions and/or prey preferences, may have played a role, it is possible that these striking late Pliocene to Pleistocene shifts in geographical distribution have been influenced by changes in the availability and distribution of prey, including medium to large-size cetaceans. Indeed, the latter were

very common in the Pliocene of the southern North Sea (e.g., Van Beneden 1880; Misonne 1958), in strong contrast with their present-day near absence in this area (van der Meij and Camphuijsen 2006; Haelters et al. 2018). In view of the global warming context and the presence of seal populations along the coast of Belgium and the Netherlands, the return of *C. carcharias* to the southern North Sea has for example been considered (Engels and Soeryanto 2025).

New chronostratigraphic data on late Neogene and Pleistocene balaenids and monodontids (e.g., Mol et al. 2006; Duboys de Lavigerie et al. 2020) from the southern North Sea will be needed to further refine the timing of the disappearance of these two groups in this region, also taking into account recent human activities (e.g., van den Hurk et al. 2022). Together with the future description and interpretation of other fossil records of trophic interactions between sharks and cetaceans, this will allow testing the potential link between these local marine mammal extinctions and the loss of large predatory sharks from the southern North Sea.

Acknowledgements

This work is dedicated to the memory of Paul Gigase (1930–2021), a very careful and cooperative avocational palaeontologist who contributed to improving our knowledge of the marine vertebrate faunas of the Belgian Neogene and generously donated the studied monodontid specimen to the RBINS. This study benefited from the DIGIT program, for the micro-CT imaging of RBINS M.1922 and RBINS M.2344, executed by Camille Locatelli (RBINS), who is warmly thanked. Object Research Systems (ORS, www.theobjects.com) and GOM Gmbh (www.gom.com) are acknowledged for providing non-commercial access to their Dragonfly ORS and GOM Inspect (version 2019) software packages. We wish to thank Nadine Müller and her team at NMB for extremely efficiently organizing the loan and transportation of the holotype cranium of *Balaenella brachyrhynus* to the RBINS, Stéphane Berton (RBINS) for his valuable help during the handling and final preparation of the cranium of the holotype of *B. brachyrhynus*, Sabine Van Cauwenberghe (Ghent University, Belgium) for the palynological maceration of the sediment sample, Alberto Collareta (Università di Pisa, Italy) for the preliminary discussion on the identification of shark tooth fragments, and Sami Mili (Institut Supérieur de la Pêche et de l'Aquaculture de Bizerte, Tunisia) for sharing detailed morphometrics of modern *Hexanchus griseus*. We also wish to thank the two reviewers, Stephen Godfrey (Calvert Marine Museum, Solomons, USA) and Giovanni Serafini (Università di Modena e Reggio Emilia, Modena, Italy), for their constructive comments and suggestions on an earlier version of this work.

Editor: Eli Amson

References

Adnet, S. and Martin, R. 2007. Increase of body size in sixgill sharks with change in diet as a possible background of their evolution. *Historical Biology* 19: 279–289.

Afonso, A.S., Macena, B.C., Mourato, B., Bezerra, N.P., Mendonca, S., de Queiroz, J.D., and Hazin, F.H. 2022. Trophic-mediated pelagic habitat structuring and partitioning by sympatric elasmobranchs. *Frontiers in Marine Science* 9: 779047.

Andrews, K.S., Williams, G.D., Farrer, D., Tolimieri N., Harvey C. J., Bargmann, G., and Levin P.S. 2009. Diel activity patterns of sixgill sharks *Hexanchus griseus*: the ups and downs of an apex predator. *Animal Behaviour* 78: 525–536.

Arnold, P.W. 1972. Predation on harbour porpoise, *Phocoena phocoena*, by a white shark, *Carcharodon carcharias*. *Journal of the Fisheries Board of Canada* 29: 1213–1214.

Assemat, A., Adnet, S., Bayez, K., Hassler, A., Arnaud-Godet, F., Mollen, F.H., Girard, C., and Martin, J.E. 2024. Exploring diet shifts and ecology in modern sharks using calcium isotopes and trace metal records of their teeth. *Journal of Fish Biology* 105: 1469–1481.

Baldanza, A., Pasini, G., Garassino, A., Carosi, A., Reichenbacher, B., Lorenzoni, M., Famiani, F., and Bizzarri, R. 2025. Scavengers and opportunists at work on whale carcasses: Decapods, echinoids and fishes. *Palaeontologia Electronica* 28 (3): 1–33.

Beck, B. and Mansfield, A.W. 1969. Observations on the Greenland shark, *Somniosus microcephalus*, in northern Baffin Island. *Journal of the Fisheries Research Board of Canada* 26: 143–145.

Benites-Palomino, A., Velez-Juarbe, J., Altamirano-Sierra, A., Collareta, A., Carrillo-Briceño, J.D., and Urbina, M. 2022. Sperm whales (Physeteroidea) from the Pisco Formation, Peru, and their trophic role as fat sources for late Miocene sharks. *Proceedings of the Royal Society B* 289: 20220774.

Benites-Palomino, A., Aguirre-Fernández, G., Velez-Juarbe, J., Carrillo-Briceño, J.D., Sánchez, R., and Sánchez-Villagra, M.R. 2023. Trophic interactions of sharks and crocodylians with a sea cow (Sirenia) from the Miocene of Venezuela. *Journal of Vertebrate Paleontology* 43 (6): e2381505.

Bianucci, G., Sorce, B., Storai, T., and Landini, W. 2010. Killing in the Pliocene: shark attack on a dolphin from Italy. *Palaeontology* 53: 457–470.

Bianucci, G., Pesci, F., Collareta, A., and Tinelli, C. 2019. A new Monodontidae (Cetacea, Delphinoidea) from the lower Pliocene of Italy supports a warm-water origin for narwhals and white whales. *Journal of Vertebrate Paleontology* 39 (3): e1645148.

Bisconti, M. 2005. Skull morphology and phylogenetic relationships of a new diminutive balaenid from the Lower Pliocene of Belgium. *Palaeontology* 48: 793–816.

Bisconti, M. and Bosselaers, M. 2016. *Fragilicetus velponi*: a new mysticete genus and species and its implications for the origin of Balaenopteridae (Mammalia, Cetacea, Mysticeti). *Zoological Journal of the Linnean Society* 177: 450–474.

Bisconti, M., Lambert, O., and Bosselaers, M. 2017. Revision of "*Balaena" belgica* reveals a new right whale species, the possible ancestry of the northern right whale, *Eubalaena glacialis*, and the ages of divergence for the living right whale species. *PeerJ* 5: e3464.

Bisconti, M., Pellegrino, L., and Carnevale, G. 2021. Evolution of gigantism in right and bowhead whales (Cetacea: Mysticeti: Balaenidae). *Biological Journal of the Linnean Society* 134: 498–524.

Bogan, S., Agnolin, F.L., and Novas, F.E. 2016. New selachian records from the Upper Cretaceous of southern Patagonia: paleobiogeographical implications and the description of a new taxon. *Journal of Vertebrate Paleontology* 36 (3): e1105235.

Bor, T.J. and Peeters, W.J.M. 2015. The Pliocene locality Balgoy (province of Gelderland, The Netherlands) and a new record of the great white shark, *Carcharodon carcharias* (Linnaeus, 1758). *Caenozoic Research* 15: 59–73.

Breed, G.A. 2021. Predators and impacts of predation. *In*: J.C. George and J.G.M. Thewissen (eds.), *The Bowhead Whale* Balaena mysticetus*: Biology and Human Interactions*, 457–470. Academic Press, London.

Brodie, P.F. 1989. The white whale *Delphinapterus leucas* (Pallas, 1776). *In*: S.H. Ridgway and R. Harrison (eds.), *Handbook of Marine Mammals, Vol. 4: River Dolphins and the Larger Toothed Whales*, 118–144. Academic Press, London.

Buono, M.R., Fernández, M.S., Cozzuol, M.A., Cuitiño, J.I., and Fitzgerald, E.M. 2017. The early Miocene balaenid *Morenocetus parvus* from Patagonia (Argentina) and the evolution of right whales. *PeerJ* 5: e4148.

Cappetta, H. 1986. Types dentaires adaptatifs chez les Sélaciens actuels et post-Paléozoiques. *Palaeovertebrata* 16 (2): 57–76.

Cappetta, H. 2006. Elasmobranchii post-Triadici (Index specierum et generum). *In*: W. Reigraf (ed.), *Fossilium catalogus I: Animalia, Pars 142*, 472 pp. Backhuys publishers, Leiden.

Cigala-Fulgosi, F. 1990. Predation (or possible scavenging) by a great white shark on an extinct species of bottlenosed dolphin in the Italian Pliocene. *Tertiary Research* 12: 17–36.

Coffey, D.M., Royer, M.A., Meyer, C.G., and Holland, K.N. 2020. Diel patterns in swimming behavior of a vertically migrating deepwater shark, the bluntnose sixgill (*Hexanchus griseus*). *PLoS One* 15 (1): e0228253.

Collareta, A., Lambert, O., Landini, W., Di Celma, C., Malinverno, E., Varas-Malca, R., Urbina, M., and Bianucci, G. 2017a. Did the giant extinct shark *Carcharocles megalodon* target small prey? Bite marks on marine mammal remains from the late Miocene of Peru. *Palaeogeography, Palaeoclimatology, Palaeoecology* 469: 84–91.

Collareta, A., Landini, W., Chacaltana, C., Valdivia, W., Altamirano Sierra, A., Urbina Schmitt, M., and Bianucci, G. 2017b. A well preserved skeleton of the fossil shark *Cosmopolitodus hastalis* from the late Miocene of Peru, featuring fish remains as fossilized stomach contents. *Rivista Italiana di Paleontologia e Stratigrafia* 123: 11–22.

Corkeron, P.J., Morris, R.J., and Bryden, M.M. 1987. Interactions between bottlenose dolphins and sharks in Moreton Bay, Queensland. *Aquatic Mammals* 13 (3): 109–113.

Deckers, J. and Louwye, S. 2020. The architecture of the Kattendijk Formation and the implications on the early Pliocene depositional evolution of the southern margin of the North Sea Basin. *Geologica Belgica* 23: 323–331.

Deméré, T.A. and Cerutti, R.A. 1982. A Pliocene shark attack on a cethotheriid whale. *Journal of Paleontology* 56: 1480–1482.

De Schepper, S. and Head, M.J. 2008. Age calibration of dinoflagellate cyst and acritarch events in the Pliocene–Pleistocene of the eastern North Atlantic (DSDP Hole 610A). *Stratigraphy* 5: 137–161.

De Schepper, S., Head, M.J., and Louwye, S. 2009. Pliocene dinoflagellate cyst stratigraphy, palaeoecology and sequence stratigraphy of the Tunnel-Canal Dock, Belgium. *Geological Magazine* 146: 92–112.

Di Beneditto, A.P.M. 2004. Presence of franciscana dolphin (*Pontoporia blainvillei*) remains in the stomach of a tiger shark (*Galeocerdo cuvieri*) captured in Southeastern Brazil. *Aquatic Mammals* 30: 311–314.

Duboys de Lavigerie, G., Bosselaers, M., Goolaerts, S., Park, T., Lambert, O., and Marx, F.G. 2020. New Pliocene right whale from Belgium informs balaenid phylogeny and function. *Journal of Systematic Palaeontology* 18: 1141–1166.

Dybkjær, K. and Piasecki, S. 2010. Neogene dinocyst zonation for the eastern North Sea Basin, Denmark. *Review of Palaeobotany and Palynology* 161: 1–29.

Ebert, D.A. 1994. Diet of the sixgill shark *Hexanchus griseus* off southern Africa. *South African Journal of Marine Science* 14: 213–218.

Ebert, D.A. and Stehmann, M.F.W. 2013. Sharks, batoids and chimaeras of the north Atlantic. *FAO Species Catalogue for Fishery Purposes* 7: 1–523.

Ehret, D.J., MacFadden, B.J., and Salas-Gismondi, R. 2009. Caught in the act: Trophic interactions between a 4-million-year-old white shark (*Carcharodon*) and mysticete whale from Peru. *Palaios* 24: 329–333.

Engels, T. and Soeryanto, A. 2025. Hoe ziet de Noordzee er in 2050 uit? *Knack* June 4th, 2025: 40–41.

Galatius, A. and Kinze, C.C. 2003. Ankylosis patterns in the postcranial skeleton and hyoid bones of the harbour porpoise (*Phocoena phocoena*) in the Baltic and North Sea. *Canadian Journal of Zoology* 81: 1851–1861.

Godfrey, S.J., Ellwood, M., Groff, S., and Scott Verdin, M. 2018. *Carcharocles*-bitten odontocete caudal vertebrae from the Coastal Eastern United States. *Acta Palaeontologica Polonica* 63: 463–468.

Godfrey, S.J., Nance, J.R., and Riker, N.L. 2021. *Otodus*-bitten sperm whale tooth from the Neogene of the Coastal Eastern United States. *Acta Palaeontologica Polonica* 66: 599–603.

Godfrey, S.J., Perez, V.J., Jones, M., Chapman, P.F., Spencer, N., and Osborne, J.E. 2025. New light on the trophic ecology of *Carcharodon hastalis* from teeth embedded in Miocene cetacean vertebrae from Calvert Cliffs in Maryland, USA. *Acta Palaeontologica Polonica* 70: 329–337.

Govender, R. and Chinsamy, A. 2013. Early Pliocene (5 Ma) shark–cetacean trophic interaction from Langebaanweg, western coast of South Africa. *Palaios* 28: 270–277.

Haelters, J., Kerckhof, F., and Jauniaux, T. 2018. Strandings of cetaceans in Belgium from 1995 to 2017. *Lutra* 61: 107–126.

Heithaus, M.R. 2001. Predator-prey and competitive interactions between sharks (order Selachii) and dolphins (suborder Odontoceti): a review. *Journal of Zoology* 253: 53–68.

Herman, J. 1975. Quelques restes de sélaciens récoltés dans les Sables du Kattendijk à Kallo. I. Selachii – Euselachii. *Bulletin de la Société Belge de Géologie* 83: 15–31.

Ichishima, H., Furusawa, H., Tachibana, M., and Kimura, M. 2019. First monodontid cetacean (Odontoceti, Delphinoidea) from the early Pliocene of the north-western Pacific Ocean. *Papers in Palaeontology* 5: 323–342.

in 't Hout, W. 1985. Haaietanden and andere Tertiaire visresten uit Kallo (België). *Gea* 18 (4): 125–144.

Jambura, P.L., Türtscher, J., Kindlimann, R., Metscher, B., Pfaff, C., Stumpf, S., Weber, G.W., and Kriwet, J. 2020. Evolutionary trajectories of tooth histology patterns in modern sharks (Chondrichthyes, Elasmobranchii). *Journal of Anatomy* 236: 753–771.

Klug, C., Schweigert, G., Hoffmann, R., Weis, R., and De Baets, K. 2021. Fossilized leftover falls as sources of palaeoecological data: a 'pabulite' comprising a crustacean, a belemnite and a vertebrate from the Early Jurassic Posidonia Shale. *Swiss Journal of Palaeontology* 140: 10.

Lambert, O. and Gigase, P. 2007. A monodontid cetacean from the Early Pliocene of the North Sea. *Bulletin de l'Institut royal des Sciences naturelles de Belgique, Sciences de la Terre* 77: 197–210.

Leriche, M. 1926. Les poissons tertiaires de Belgique. IV. Les poissons néogènes. *Mémoires du Musée Royal d'Histoire Naturelle de Belgique* 32: 367–472.

Long, D.J. and Jones, R.E. 1996. White shark predation and scavenging on cetaceans in the eastern North Pacific Ocean. *In*: A.P. Klimley and D.G. Ainley (eds.), *Great White Sharks: The Biology of* Carcharodon carcharias, 293–307. Academic Press, London.

Louwye, S., Head, M.J., and De Schepper, S. 2004. Dinoflagellate cyst stratigraphy and palaeoecology of the Pliocene in northern Belgium, southern North Sea Basin. *Geological Magazine* 141: 353–378.

Marquet, R. 1995. Pliocene gastropod faunas from Kallo (Oost-Vlaanderen, Belgium). Part 1. Introduction and Archaeogastropoda. *Contributions to Tertiary and Quaternary Geology* 32 (1–3): 53–85.

Marx, F.G. and Lambert, O. 2021. Fossil record. *In*: J.C. George and J.G.M. Thewissen (eds.), *The Bowhead Whale* Balaena mysticetus*: Biology and Human Interactions*, 11–17. Academic Press, London.

MacNeil, M.A., McMeans, B.C., Hussey, N.E., Vecsei, P., Svavarsson, J., Kovacs, K.M., Lydersen, C., Treble, M.A., Skomal, G.B., Ramsey, M., and Fisk, A.T. 2012. Biology of the Greenland shark *Somniosus microcephalus*. *Journal of Fish Biology* 80: 991–1018.

McKenna, M.F., Cranford, T.W., Berta, A., and Pyenson, N.D. 2012. Morphology of the odontocete melon and its implications for acoustic function. *Marine Mammal Science* 28: 690–713.

McNeil, B., Lowry, D., Larson, S., and Griffing, D. 2016. Feeding behavior of subadult sixgill sharks (*Hexanchus griseus*) at a bait station. *PLoS ONE* 11 (5): e0156730.

Mead, J.G. and Fordyce, R.E. 2009. The therian skull: a lexicon with emphasis on the odontocetes. *Smithsonian Contributions to Zoology* 627: 1–248.

Merella, M., Collareta, A., Casati, S., Di Cencio, A., and Bianucci, G. 2021. An unexpected deadly meeting: deep-water (hexanchid) shark bite marks on a sirenian skeleton from Pliocene shoreface deposits of Tuscany (Italy). *Neues Jahrbuch für Geologie und Paläontologie Abhandlungen* 301: 295–305.

Merella, M., Collareta, A., Casati, S., Di Cencio, A., and Bianucci, G. 2022a. Erratum: Merella, M., Collareta, A., Casati, S. Di Cencio, A. and Bianucci, G. (2021): An unexpected deadly meeting: deep-water (hexanchid) shark bite marks on a sirenian skeleton from Pliocene shoreface deposits of Tuscany (Italy). *Neues Jahrbuch für Geologie und Paläontologie Abhandlungen* 303: 239–241.

Merella, M., Collareta, A., Granata, V., Casati, S., and Bianucci, G. 2022b. New remains of *Casatia thermophila* (Cetacea, Monodontidae) from the lower Pliocene marine vertebrate-bearing locality of Arcille (Tuscany, Italy). *Rivista Italiana di Paleontologia e Stratigrafia* 128: 229–240.

Mili, S., Ghanem, R., Ennouri, R., Troudi, D., Zarrouk, H., and Jabbari, S. 2021. Biological aspects of the Bluntnose sixgill shark, *Hexanchus griseus* (Bonnaterre, 1788) in Tunisian waters: implications for fishery management. *Journal of New Sciences* 15: 333–345.

Misonne, X. 1958. Faune du Tertiaire et du Pléistocène inférieur de Belgique (Oiseaux et Mammifères). *Bulletin de l'Institut Royal des Sciences Naturelles de Belgique* 34 (5): 1–36.

Mol, D., Post, K., Reumer, J. W. F., van der Plicht, J., de Vos, J., van Geel, B., van Reenen, G., Pals, J. P., & Glimmerveen, J. 2006. The Eurogeul –first report of the palaeontological, palynological and archaeological investigations of this part of the North Sea. *Quaternary International* 142–143: 178–185.

Monteiro, M.S., Vaske Jr, T., Barbosa, T.M., and Alves, M.D.O. 2006. Predation by a shortfin mako shark, *Isurus oxyrinchus*, Rafinesque, 1810, on a pantropical spotted dolphin, *Stenella atenuatta* [sic], calf in Central Atlantic waters. *Latin American Journal of Aquatic Mammals* 5: 141–144.

Moore, M.J., Mitchell, G.H., Rowles, T.K., and Early, G. 2020. Dead cetacean? Beach, bloat, float, sink. *Frontiers in Marine Science* 7: 333.

Moran, M.M., Bajpai, S., George, J.C., Suydam, R., Usip, S., and Thewissen, J.G.M. 2015. Intervertebral and epiphyseal fusion in the postnatal ontogeny of cetaceans and terrestrial mammals. *Journal of Mammalian Evolution* 22: 93–109.

Mucientes, G., Vilas-Arrondo, N., and Villegas-Ríos, D. 2025. Do shortfin mako *Isurus oxyrinchus* hunt dolphins actively? *Journal of Fish Biology* [published online https://doi.org/10.1111/jfb.70113]

Muñiz, F., Belaústegui, Z., Toscano, A., Ramirez-Cruzado, S., and Gámez Vintaned, J.A. 2020. New ichnospecies of *Linichnus* Jacobsen & Bromley, 2009. *Ichnos* 27: 344–351.

Nielsen, J., Christiansen, J.S., Grønkjær, P., Bushnell, P., Steffensen, J.F., Kiilerich, H.O., Præbel, K., and Hedeholm, R. 2019. Greenland shark (*Somniosus microcephalus*) stomach contents and stable isotope values reveal an ontogenetic dietary shift. *Frontiers in Marine Science* 6: 125.

Nijssen, H. and De Groot, S. J. 1980. Zeevissen van de Nederlandse kust. *Wetenschappelijke mededelingen van de Koninklijke Nederlandse Natuurhistorische Vereniging* 143: 1–109.

Nolf, D. 1988. *Fossiles de Belgique: dents de requins et de raies du tertiaire de la Belgique*. 184 pp. Institut royal des Sciences naturelles de Belgique, Brussels.

Nowacek, D.P., Johnson, M.P., Tyack, P.L., Shorter, K.A., McLellan, W.A., and Pabst, D.A. 2001. Buoyant balaenids: the ups and downs of buoyancy in right whales. *Proceedings of the Royal Society B* 268: 1811–1816.

Nuyts, H. 1990. Note on the biostratigraphy (benthic foraminifera) and lithostratigraphy of Pliocene deposits at Kallo (Oost-Vlaanderen; Belgium). *Contributions to Tertiary and Quaternary Geology* 27: 17–25.

Poll, M. 1947. *Faune de Belgique. Poissons marins*. 452 pp. Institut royal des Sciences naturelles de Belgique, Brussels.

Post, K. 1999. Laat-pleistocene zeezoogdieren van de Nederlandse kustwateren. *Grondboor & Hamer* 53 (6): 126–130.

Rappé, G. and Eneman, E. 1988. *De zeevissen van België*. 48 pp. De Strandwerkgroep, Ostend.

Receveur, A., Allain, V., Menard, F., Lebourges Dhaussy, A., Laran, S., Ravache, A., Bourgeois, K., Vidal, E., Hare, S.R., Weimerskirch, H., Borsa, P., and Menkes, C. 2022. Modelling marine predator habitat using the abundance of its pelagic prey in the tropical South-Western Pacific. *Ecosystems* 25: 757–779.

Richard, J.T., Pellegrini, I., and Levine, R. 2024. Belugas (*Delphinapterus leucas*) create facial displays during social interactions by changing the shape of their melons. *Animal Cognition* 27: 7.

Serafini, G., Danise, S., Maxwell, E.E., Martire, L., Amalfitano, J., Miriam, C., Thun Hohenstein, U., and Giusberti, L. 2024. Of his bones are crinoid made: taphonomy and deadfall ecology of marine reptiles from a pelagic setting (Middle–Upper Jurassic of Northeastern Italy). *Rivista Italiana di Paleontologia e Stratigrafia* 130 97–128.

Shimada, K. 1997. Paleoecological relationships of the Late Cretaceous lamniform shark, *Cretoxyrhina mantelli* (Agassiz). *Journal of Paleontology* 71: 926–933.

Smitz, H. 2011. *De ontwikkeling van de haven van Antwerpen de voorbije 75 jaar en de relatie tot de Scheldepolders deel 1*. 147 pp. Waterbouwkunding Laboratorium 1933–2009, Antwerp.

Taylor, J.K.D., Mandelman, J.W., McLellan, W.A., Moore, M.J., Skomal, G.B., Rotstein, D.S., and Kraus, S.D. 2013. Shark predation on North Atlantic right whales (*Eubalaena glacialis*) in the southeastern United States calving ground. *Marine Mammal Science* 29: 204–212.

Terranova, E., Bianucci, G., Merella, M., Sorbini, C., and Collareta, A. 2025. Retrieving palaeoecological information from historic fossil finds: a taphonomic cold case from Orciano Pisano (Central Italy) reveals a distinctive trophic interaction in the Pliocene Mediterranean Sea. *Journal of Marine Science and Engineering* 13: 508.

Tucker, J.P., Vercoe, B., Santos, I.R., Dujmovic, M., and Butcher, P.A. 2019. Whale carcass scavenging by sharks. *Global Ecology and Conservation* 19: e00655.

Van Beneden, P.-J. 1880. Description des ossements fossiles des environs d'Anvers. Deuxième partie. Cétacés. Genres *Balaenula*, *Balaena* et *Balaenotus*. *Annales du Musée Royal d'Histoire Naturelle de Belgique* 4: 1–82.

Van den Hurk, Y., Spindler, L., McGrath, K., and Speller, C. 2022. Medieval whalers in the Netherlands and Flanders: zooarchaeological analysis of medieval cetacean remains. *Environmental Archaeology* 27: 243–257.

Van der Meij, S.E. and Camphuijsen, C.J. 2006. Distribution and diversity of whales and dolphins (Cetacea) in the Southern North Sea 1970–2005. *Lutra* 49: 3–28.

van Netten, H.H. and Reumer, J.W.F. 2009. Bite marks on early Holocene *Tursiops truncatus* fossils from the North Sea indicate scavenging by rays (Chondrichthyes, Rajidae). *Netherlands Journal of Geosciences* 88 (3): 169-175.

Vélez-Juarbe, J. and Pyenson, N.D. 2012. *Bohaskaia monodontoides*, a new monodontid (Cetacea, Odontoceti, Delphinoidea) from the Pliocene of the western North Atlantic Ocean. *Journal of Vertebrate Paleontology* 32: 476–484.

Wilga, C.D. 2002. A functional analysis of jaw suspension in elasmobranchs. *Biological Journal of the Linnean Society* 75: 483–502.

Würsig, B., Thewissen, J.G.M., and Kovacs, K.M. 2018. *Encyclopedia of Marine Mammals.* Third edition, 1157 pp. Academic Press, London.